# RETRACTED: Upregulation of C Terminus of Hsc70-Interacting Protein Attenuates Apoptosis and Procoagulant Activity and Facilitates Brain Repair After Traumatic Brain Injury

Hao Chen[1], Yao Jing[1], Zhiming Xu[1], Dianxu Yang[1], Shiming Ju[1], Yan Guo[1], Hengli Tian[1] and Lixia Xue[2]*

[1] Department of Neurosurgery, Shanghai Jiao Tong University Affiliated Sixth People's Hospital, Shanghai, China,
[2] Department of Neurology, Shanghai Jiao Tong University Affiliated Sixth People's Hospital, Shanghai, China

Traumatic brain injury (TBI) could highly induce coagulopathy through breaking the dynamic balance between coagulation and fibrinolysis systems, which may be a major contributor to the progressive secondary injury cascade that occurs after TBI. Phosphatase and tensin homolog deleted on chromosome 10 (PTEN) inhibition is reported to exert neuroprotection in TBI, making it a potential regulatory target involved in TBI-induced coagulation disorder. PTEN level is controlled in a major way by E3 ligase-mediated degradation through the ubiquitin–proteasome system. The C terminus of Hsc70-interacting protein (CHIP) has been shown to regulate proteasomal degradation and ubiquitination level of PTEN. In the present study, CHIP was overexpressed and knocked down in mouse brain microvascular endothelial cells (bEnd.3) and tissues during the early phase of TBI. *In vitro* cell proliferation, cell apoptosis, migration capacity, and invasion capacity were determined. The changes of procoagulant and apoptosis molecules after TBI were also detected as well as the micrangium density and blood–brain barrier permeability after *in vivo* TBI. *In vitro* results demonstrated that CHIP overexpression facilitated bEnd.3 cell proliferation, migration, and invasion and downregulated cell apoptosis and the expressions of procoagulant molecules through promoting PTEN ubiquitination in a simulated TBI model with stretch-induced injury treatment. *In vivo* experiments also demonstrated that CHIP overexpression suppressed post-TBI apoptosis and procoagulant protein expressions, as well as increased microvessel density, reduced hemorrhagic injury, and blood–brain barrier permeability. These findings suggested that the upregulation of CHIP may attenuate apoptosis and procoagulant activity, facilitate brain repair, and thus exerts neuroprotective effects in TBI.

Keywords: traumatic brain injury, coagulopathy, phosphatase and tensin homolog deleted on chromosome 10, C terminus of Hsc70-interacting protein, apoptosis, procoagulant activity

# INTRODUCTION

Traumatic brain injury (TBI) is an important public health problem worldwide. It is a major cause of morbidity and mortality, which is greatly contributed by the concomitant of coagulation disorders to brain injury (Zhang et al., 2012). Numerous literatures have shown that abnormalities in blood coagulation commonly developed after TBI, which led to various delayed or progressive secondary brain injuries including hemorrhage, ischemia/infarction, as well as enlargement of previously small hemorrhagic lesions (Stein et al., 1992, 1993; Carrick et al., 2005). Progressive hemorrhagic injury (PHI), one of the most important and devastating complications after initial brain injury, is reported to be significantly associated with trauma-induced coagulopathy (TIC) (Maegele, 2013; Yang et al., 2014; de Oliveira Manoel et al., 2015). Our previous studies demonstrated that the risk of PHI after TBI can be predicted by some parameters of coagulopathy, including high D-dimer level, prolonged prothrombin time (PT), or low platelet count (Tian et al., 2010; Yuan et al., 2012; Liu and Tian, 2016). Post-traumatic cerebral infarction (PTCI) is also a severe secondary brain injury after TBI, with a reported incidence ranging from 1.9 to 18.8% (Server et al., 2001; Marino et al., 2006; Tawil et al., 2008; Tian et al., 2008; Liu et al., 2015). A good correlation between microthrombosis formation and post-traumatic cerebral ischemia/PTCI has been confirmed by histopathological findings (Stein et al., 2004; Schwarzmaier et al., 2010). In our previous clinical study, the mentioned coagulopathy parameters (elevated D-dimer, abnormal PT, and thrombocytopenia), or disseminated intravascular coagulation scores, which also reflect thrombus formation, were each independently associated with an increased risk of PTCI, further indicating that TIC was also associated with post-traumatic cerebral ischemia (Chen et al., 2013).

Under normal circumstances, the coagulation system and fibrinolysis system maintain a dynamic balance to ensure unobstructed blood flow and post-injury hemostasis. It is well-known that TBI can cause the early activation of the procoagulant system through the generation of procoagulant microparticles and their downstream effects (Morel et al., 2008; De Luca et al., 2017). Several procoagulation activators, such as tissue factor (TF) (Barklin et al., 2009) and von Willebrand factor (vWF) (De Oliveira et al., 2007), are released from the injured brain microvascular endothelial cells (BMVECs) and enhance blood coagulation after TBI. Platelet-endothelial adhesion molecule-1 (PECAM-1) is also secreted by BMVECs, is involved in the adhesion of neutrophils to the endothelium, and is inducing thrombus formation (Carlos et al., 1997). Plasminogen activator inhibitor-1 (PAI-1), as the principal inhibitor of the activation of plasminogen and fibrinolysis, also increases the risks for coagulopathy after TBI (Condron et al., 2018). The molecular regulation mechanisms of coagulation disorder after TBI has not been fully elucidated. Phosphoinositide 3-kinase–AKT pathway has been considered to play a crucial role in regulating the coagulation and fibrinolysis (Schabbauer et al., 2004; Hori et al., 2005). Phosphatase and tensin homolog deleted on chromosome 10 (PTEN),

the major negative regulator of AKT signaling (Song et al., 2012), is thus speculated to be involved in the coagulation disorder after TBI.

Currently, evidences suggested that PTEN/AKT pathway contributes to neuroprotection in TBI. It has been reported that promoting PTEN/AKT signaling alleviated apoptosis of cortical neurons and improved the neurological outcome *in vitro* after experimental TBI (Ge et al., 2014; Han et al., 2014). We have reported that PTEN phosphorylation induced by bisperoxovanadium reduced neurological damage, decreased blood–brain barrier (BBB) permeability, and enhanced angiogenesis after TBI and ischemic brain injury in our previous studies (Ding et al., 2013; Guo et al., 2013; Xue et al., 2018). Besides phosphorylation, ubiquitination is known as another important post-translational modification of PTEN, and PTEN level is mainly controlled by E3 ligase-mediated degradation through the ubiquitin–proteasome system (Voutsadakis, 2012; Shao et al., 2017; Kao et al., 2018). As a chaperone-associated E3 ligase, the C terminus of Hsc70-interacting protein (CHIP) is reported to induce PTEN ubiquitination and regulate the proteasomal turnover of PTEN (Ahmed et al., 2012). Overexpression of CHIP leads to elevated PTEN ubiquitination and a shortened half-life of endogenous PTEN. In contrast, depletion of endogenous CHIP stabilizes PTEN (Xu T. et al., 2017). Thus, this present study attempted to regulate CHIP expression after TBI through the overexpression and interference technology, to further explore the role and potential mechanism of CHIP in TBI-induced early coagulopathy, the maintenance of BMVECs function, and brain injury repair after TBI, thereby providing theoretical basis for the treatment of secondary brain injury after TBI.

# MATERIALS AND METHODS

## Cell Culture

The mouse BMVEC line (bEnd.3 cells) was purchased from the American Type Culture Collection, Manassas, VA, United States. Cells were cultured in Roswell Park Memorial Institute-1640 medium (Gibco Laboratories; Grand Island, NY, United States) supplemented with 10% fetal bovine serum (FBS), streptomycin (100 µg/ml), and penicillin (100 µg/ml) at 37°C in a humidified incubator with 5% carbon dioxide and 95% air. For the experiments, the cells were seeded at a density of 0.14–$0.6 \times 10^5$/cm$^2$ in BioFlexR culture plates (Flexcell International Corp.; Burlington, NC) or collagen-coated glass coverslips.

## Plasmid Constructions and Cell Transfection

To generate stable expression and interference constructions, polymerase chain reaction (PCR)-amplified mouse CHIP and short hairpin (sh) RNA1, shRNA2, shRNA3, and shRNA4 were cloned into lentivirus expression vectors, which contained green fluorescent protein to indicate transfection efficiency, detailed information for shRNA is provided in **Table 1**. bEnd.3 cells were seeded into a 12-well plate at $5 \times 10^4$ cells and infected with lentivirus at a multiplicity of infection of 100. After

| shRNA name | Clone ID | Target sequence |
| --- | --- | --- |
| shRNA 1 | – | GCTGGAGATGGAGAGTTATGA |
| shRNA 2 | – | GAGCCTATAGTTTGGCCAAGG |
| shRNA 3 | – | GAGATATCCCTGACTACTTGT |
| shRNA 4 | – | GCATTACACCCAGTGGTATCA |

CHIP, C terminus of Hsc70-interacting protein.

48 h, the medium of infected bEnd.3 cells were changed into normal medium containing 5-μg/ml puromycin to screening the stable expression cell lines. The clones were confirmed by immunoblotting and divided into control, corresponding negative control for CHIP overexpression (NC-OE), CHIP overexpression (CHIP-OE), shRNA negative control (NC-shRNA), and CHIP knockdown (shRNA) groups. Stable cell lines were maintained in minimal essential medium supplemented with 10% FBS and 2-μg/ml puromycin.

## *In vitro* Stretch Model

*In vitro* simulated TBI was induced by the mechanical injury device in cultured bEnd.3 cells as described previously (Yuan et al., 2016; Xu Z. M. et al., 2017; Liu et al., 2018; Yang et al., 2019). Cells were grown in Bioflex cell culture wells with 2-mm-thick silastic membranes (Flexcell International Corp) for 24 h. A biaxial stretch injury was applied to the cells using the Cell Injury Controller II system (Virginia Commonwealth University), which can exert a rapid positive pressure of known amplitude (pounds per square inch) and duration (millisecond). A controllable, with 4.8 psi, pressure pulse for 50 ms was used to transiently deform the silastic membrane and, thus stretch the cells growing on the membrane, was proportional to the amplitude and duration of the air pressure pulse. This degree of stretch injury is thought to be analogous to the range of mechanical stress exerted on the human brain after rotational acceleration–deceleration injuries (Ellis et al., 1995; McKinney et al., 1996). After *in vitro* stretch-induced injury treatment, cells were incubated for an additional 24 h before the following biological researches.

## Cell Proliferation Assay

The CCK-8 assay was used to determine bEnd.3 cells viability following *in vitro* stretch-induced injury treatment. Cells were seeded at a density of $5 \times 10^4$ cells/well in Bioflex 6-well plates for 12 h after stretch-induced injury. After relevant culture time, cell viability was measured using a CCK-8 kit (Dojindo Laboratories) according to the manufacturer's instructions. CCK-8 solution (100 μl) was added to 900 μl of culture media and incubated for 3 h at 37°C in a humidified atmosphere of 5% carbon dioxide. The optical density (OD) was measured at 450 nm in a microplate reader. The experiment was performed in triplicate at different times.

## Flow Cytometric Analysis of Apoptosis

Annexin V-FITC Apoptosis Detection Kit (BD) was used to evaluate the percentage of apoptotic cells. Cells were seeded in Bioflex 6-well plates for 24 h after stretch-induced injury. Treated cells ($5 \times 10^5$/ml) were centrifuged and resuspended in cold $1\times$ binding buffer, next, 5-μl Annexin V-FITC, and 10-μl propidium iodide (PI) (P3566, Thermo Fisher Scientific, United States) was added, and the suspension was analyzed by fluorescence-activated cell sorting (FACS) cytometry (Beckman). For each sample, at least 10,000 cells were analyzed.

## Wound Healing Test

The migration capacity of the cells was evaluated by the wound healing test. After stretch-induced injury treatment, $3 \times 10^5$ cells were seeded in the Bioflex 6-well plates for 12 h. Wounds were created in the confluent cells using a 10-μl pipette tips. Cells were then rinsed with medium to remove any free-floating cells and debris. Wound healing was observed after 0, 24, and 48 h within the scrape line, and representative scrape lines were imaged. These images were analyzed and qualified with ImageJ (Version: 1.52s) software. The wound healing rate was calculated with the 0-h area of each group as the control, the formula as follows: wound healing rate % = 100% - (area time nh/area time 0 h × 100%).

## Transwell Assay

The invasion capacity of the cells was evaluated by the transwell assay according to the manufacturer's protocol. Briefly, the upper chambers were coated with Matrigel (BD Biosciences). Cells were seeded in the Bioflex 6-well plates for 12 h after stretch-induced injury treatment. In 100-μl serum-free medium, $5 \times 10^4$ cells were then seeded in the upper chamber of a matrigel-coated transwell culture system, and 500-μl medium was added in the lower chamber with 10% FBS. The cells were then allowed to invade the Matrigel matrix for 24 h. After that, the transmigrated cells were fixed and stained with 0.1% crystal violet and counted in five randomly selected microscopic fields.

## Immunoblotting

The cells were collected and suspended in mammalian protein extraction reagent (Thermo) for at least 1 h on ice. Cell lysates were clarified by centrifugation at $12,000 \times g$ for 10 min at 4°C. The protein contents in the supernatant were measured using a Bio-Rad DC protein assay kit II (Bio-Rad). Proteins were separated by electrophoresis on 8–15% sodium dodecyl sulfate (SDS) polyacrylamide gel and electrotransferred onto a nitrocellulose filter membrane (NC membrane). It is used as the carrier of C/T line in colloidal gold test paper, and it is also the place where immune response occurs. NC membrane was blocked in 5% non-fat skim milk and probed with primary antibodies; this was followed by incubation with horseradish peroxidase-conjugated secondary antibodies. Protein expression was detected using a SuperSignal West Pico Chemiluminescence system (Pierce). The images of bands were analyzed with image analysis software (Image-Pro Plus 6.0). The antibodies against glyceraldehyde-3-phosphate dehydrogenase, CHIP, PTEN and TF were purchased from Proteintech, United States. The antibodies against AKT, phospho-AKT, caspase-3, cleaved caspase-3, cleaved caspase-8, and apoptosis-inducing factor were purchased

from Cell Signaling Technology, United States. The antibodies against vWF, PAI-1, Fas, PECAM-1, caspase-8, and ubiquitin were purchased from Abcam, United Kingdom. Detailed information of primary antibodies used in this study is provided in **Table 2**.

## *In vitro* Ubiquitylation Assay

The transfected bEnd.3 cells were treated with 20-μM proteasome inhibitor MG132 (S2619, CAS#133407-82-6, Selleck, United States) or with vehicle (dimethyl sulfoxide) for 12 h after stretch-induced injury treatment. The cells were washed with phosphate-buffered saline (PBS) and lysed in 0.5 ml of 4-(2-hydroxyethyl)-1-piperazineethanesulfonic acid (HEPES) buffer (20-mM HEPES, pH 7.2, 50-mM sodium chloride, and 1-mM sodium fluoride, 0.5% Titon-X100) supplemented with 0.1% SDS and protease-inhibitor cocktail (Roche, Germany). The lysates were centrifuged to obtain cytosolic proteins. Briefly, cell lysates were incubated with antibody against PTEN at 4°C overnight, followed by addition of protein A/G Sepharose beads (Sigma). After 3 h, the beads

were collected, washed three times with HEPES buffer, resolved by SDS polyacrylamide gel for 10 min, and then subjected to immunoblotting.

## Animals and *in vivo* Traumatic Brain Injury Model

All animals were treated according to the international guidelines for animal research, and the animal protocol used in this study was reviewed and approved by the Institutional Animal Care and Use Committee of the Shanghai Jiao Tong University Affiliated Sixth People's Hospital. Male C57BL/6 mice (aged 6–8 weeks, with a weight of 21–25 g) were purchased (Shanghai Slac Laboratory Animal Co., Ltd.), and housed under standard nutritional and environmental conditions. Two-microliter lentiviral suspension ($5 \times 10^{12}$ IU) containing control, CHIP-OE, or interference particles was injected through unilateral cerebral ventricle microinjection (0.3 mm posterior from bregma, 1 mm lateral to the sagittal suture, and 2.5 mm below dura) at the rate of 0.2 μl/min for one mouse, 2 days before TBI model building. Controlled cortical impact (CCI)

**TABLE 2 |** Primary antibodies information.

| Name | Description of immunogen | Source, host species, catalog No., RRID | Concentration used |
|---|---|---|---|
| GAPDH (glyceraldehyde-3-phosphate dehydrogenase) | GAPDH fusion protein Ag0766 | Proteintech, Mouse Monoclonal, 60004-1-1, AB_2107436 | 1:5000 (WB) |
| CHIP (C terminus of Hsc70-interacting protein) | Peptide | Proteintech, Rabbit Polyclonal, 55430-1-AP, AB_10949225 | 1:1000 (WB) |
| PTEN (Phosphatase and tensin homolog deleted on chromosome 10) | PTEN fusion protein Ag17274 | Proteintech, Rabbit Polyclonal, 22034-1-AP, Not available | 1:5000 (WB) 4 μg (IP) 1:500 (WB) |
| TF (tissue factor) | Transferrin fusion protein Ag11504 | Proteintech, Rabbit Polyclonal, 17435-1-AP, AB_2035023 | 1:1000 (WB) |
| AKT | Synthetic peptide corresponding to the carboxy-terminal sequence of mouse Akt | Cell Signaling Technology, Rabbit Polyclonal, 9272, AB_329827 | 1:1000 (WB) |
| p-AKT (phospho-AKT) | Synthetic phosphopeptide corresponding to residues surrounding Thr308 of mouse Akt | Cell Signaling Technology, Rabbit Monoclonal, 2965, AB_2255933 | 1:1000 (WB) |
| Caspase-3 | Synthetic peptide corresponding to residues surrounding the cleavage site of human caspase-3 | Cell Signaling Technology, Rabbit Polyclonal, 9662, AB_331439 | 1:1000 (WB) |
| Cleaved caspase-3 | Synthetic peptide corresponding to amino-terminal residues adjacent to Asp175 of human caspase-3 | Cell Signaling Technology, Rabbit Monoclonal, 9664, AB_2070042 | 1:1000 (WB) |
| Cleaved caspase-8 | Synthetic peptide corresponding to residues adjacent to Asp391 of human Caspase-8 | Cell Signaling Technology, Rabbit Monoclonal, 9496, AB_561381 | 1:1000 (WB) |
| AIF (apoptosis-inducing factor) | Synthetic peptide corresponding to residues within the carboxy terminus of AIF | Cell Signaling Technology, Rabbit Polyclonal, 4642, AB_2224542 | 1:1000 (WB) |
| vWF (von Willebrand factor) | Full length native protein (purified) corresponding to Human Von Willebrand Factor | Abcam, Rabbit Polyclonal, Ab6994, AB_305689 | 1:500 (WB) |
| PAI-1 (plasminogen activator inhibitor-1) | Synthetic peptide corresponding to Human PAI1 aa 100-200 conjugated to keyhole limpet hemocyanin | Abcam, Rabbit Polyclonal, Ab66705, AB_1310540 | 1:1000 (WB) |
| Fas | Synthetic peptide (Mouse) derived from the extracellular domain, conjugated to KLH | Abcam, Rabbit Polyclonal, Ab82419, AB_1658628 | 1:1000 (WB) |
| PECAM-1 (platelet-endothelial adhesion molecule-1) | Synthetic peptide within Mouse CD31 aa 700 to the C-terminus (C terminal) | Abcam, Rabbit Polyclonal, Ab28364, AB_726362 | 1:1000 (WB) |
| Caspase-8 | Synthetic peptide corresponding to Human Caspase-8 | Abcam, Rabbit Polyclonal, Ab25901, AB_448890 | 1:500 (WB) |
| Ub (Ubiquitin) | Synthetic peptide within Human Ubiquitin aa 1-100 | Abcam, Rabbit Monoclonal, Ab134953, AB_2801561 | 1:1000 (WB) |

*WB, western blotting (immunoblotting); IP, immunoprecipitation.*

injury was adopted as *in vivo* TBI treatment as described before (Yuan et al., 2016; Xu Z. M. et al., 2017; Liu et al., 2018; Yang et al., 2019). Briefly, mice were anesthetized with sodium pentobarbital (65 mg/kg) and then placed on a heated pad to maintain their core body temperature at 37°C. A 10-mm midline incision was made over the skull, and the skin and fascia were retracted. Then, a craniotomy was performed using a 4-mm trephine over the central aspect of the right parietal bone, 1 mm lateral to the sagittal suture. The operation was performed carefully to keep the dura intact, and mice were excluded from the study if dural integrity was destroyed. The TBI was created using a rounded steel impactor tip (3 mm diameter) of a CCI device (PinPoint Precision Cortical Impactor PCI3000; Hatteras Instruments Inc., Cary, NC, United States), oriented perpendicular to the cortical surface. An injury of moderate severity was induced using an impact velocity of 1.5 m/s, deformation depth of 1.5 mm, and dwell time of 100 ms. The same procedure was performed exactly the same as that in sham animals, except that the CHIP expression intervention was not performed. All mice (total $n = 50$) were randomly divided into three groups, termed as Con group ($n = 5$), CHIP-OE group ($n = 20$), and CHIP-shRNA group ($n = 25$). All three groups were made to experience *in vivo* TBI treatment. After 0, 24, 48, and 72 h of CCI, the CHIP-OE group of mice (each subgroup $n = 5$) were killed. The CHIP-shRNA group of mice were killed after 0, 6, 24, 48, and 72 h of CCI (each subgroup $n = 5$). A 3-mm coronal tissue section from the ipsilateral cortex centering on the impact site was obtained immediately after killing.

## Immunofluorescence Analysis

Tissue samples were dewaxed with xylene, rehydrated in gradient ethyl alcohol, washed in PBS, and blocked with 1% bovine serum albumin in PBS for 30 min. Then, samples were stained with primary CD31 antibody at 4°C overnight and incubated with Alexa 488-conjugated donkey anti-mouse secondary antibody (Jackson ImmunoResearch) at 37°C for 1 h. In addition, after staining with dihydrochloride (28718-90-3, Thermo Fisher Scientific, United States), the tissue on coverslips (three slices per animal, $n = 5$ animals/subgroup) was observed under a confocal microscope (Lecia), and photomicrograph (200×) was taken at the meantime. The micrangium density (CD31 expression level) was calculated with counting the total number of CD31-positive (red fluorescent) vascular endothelial cells using ImageJ version 1.52s software.

## Hematoxylin and Eosin Staining

Tissues were immersed in 4% paraformaldehyde for 4 h, and transferred to 70% ethanol. Mouse brain biopsy material was placed in processing cassettes, dehydrated through a serial alcohol gradient, and then stained with hematoxylin and eosin. After staining, sections were dehydrated through increasing concentrations of ethanol and xylene. Then, the stained brain slices (three slices per animal) were observed under a confocal microscope, and a photomicrograph (40×) was taken. The red stained areas indicated hemorrhagic injuries

and were semi-quantified by mean OD using ImageJ (Version: 1.52s) software.

## Blood–Brain Barrier Permeability Evaluation

Immunoglobulin (Ig) G immunohistochemistry was used to evaluate the integrity of the BBB. Brain slices were rinsed with 3% hydrogen peroxide at room temperature for 30 min to eliminate endogenous peroxidase, 10% goat serum blocked at 37°C for 30 min, IgG secondary antibody (Goat Anti-Mouse IgG H&L, Abcam, Ab205719) incubated at 37°C for 1 h and AB solution (1: 200, Vector) at 37°C for 1 h, and developed color with DAB (Vector). Then, the brain slices (three slices per animal) was observed under the confocal microscope, and a photomicrograph (200×) was taken. BBB permeability was evaluated using semi-quantitative analysis of leaked IgG protein (mean OD) as determined by ImageJ version 1.52s software.

## Statistical Analysis

All images are analyzed by people who are not involved in the experiment. All statistical analyses were carried out using software SPSS 16.0. All data are presented as the mean ± standard deviation (SD). Statistical significance was determined by paired or unpaired Student t-test in cases of standardized expression data. One-way or two-way analysis of variance (ANOVA) was performed for multiple group comparisons when appropriate, and comparisons between two groups were conducted using the least significant difference method. $p < 0.05$ was considered significant. Each experiment was performed in triplicate.

## RESULTS

## Overexpression and Knockdown of C Terminus of Hsc70-Interacting Protein in bEnd.3 Cells

We firstly established the CHIP-OE and CHIP-knockdown mouse BMVEC cell lines (bEnd.3). Green fluorescence represented the cells infected by lentivirus, as shown in **Figure 1A**; cell lines were all successfully infected. The CHIP-OE cell lines have a relatively higher level confluence in comparison with NC-OE cell lines; in the contrary, shRNA1 and shRNA4 CHIP-knockdown cell lines have a significantly lower level confluence in comparison with NC-OE and NC-shRNA cell lines. The CHIP-OE cells have a spindle shape, whereas shRNA1 and shRNA4 CHIP-knockdown cells have a slimmer and irregulate shape. Immunoblotting (**Figures 1B,C**) was used to detect the protein level of CHIP in CHIP-OE and the CHIP-knockdown (shRNA1, shRNA2, shRNA3, and shRNA4) cell lines. CHIP was upregulated in CHIP-OE bEnd.3 cell lines and obviously downregulated in shRNA1, shRNA3, and shRNA4 cell lines. Considering the slow growth of shRNA3 cell line, shRNA1

**FIGURE 1 |** C terminus of Hsc70-interacting protein (CHIP) overexpression and knockdown in bEnd.3 cells. **(A)** PCR-amplified mouse CHIP and shRNA1, shRNA2, shRNA3, and shRNA4 were cloned into lentivirus expression vectors, which contained green fluorescent protein to indicate transfection efficiency. After 48 h, the transfection efficiency was observed using fluorescence microscope. NC represented non-coding control plasmid. **(B)** Protein level of CHIP after overexpression and interference was tested by immunoblotting. **(C)** CHIP/glyceraldehyde-3-phosphate dehydrogenase relative level after overexpression and interference. ***$p < 0.001$ vs. the NC-shRNA, ###$p < 0.001$ vs. the NC-OE, Scale bars: 50 μm.

and shRNA4 CHIP-knockdown bEnd.3 cell lines were cultured for the further researches.

## C Terminus of Hsc70-Interacting Protein Overexpression Promoted Cell Growth and Attenuated Apoptosis After *in vitro* Simulated Traumatic Brain Injury

In this study, bEnd.3 cells were subjected to mechanical injury to simulate the endothelial disruption that can occur in the primary injury phase of TBI. The cell proliferation and apoptosis experiments showed that CHIP-OE significantly promoted cell proliferation of bEnd.3 cells after stretch-induced injury treatment, whereas the cell proliferation of injured bEnd.3 cells was suppressed after CHIP interference (shRNA1 and shRNA4 groups) (**Figure 2A**). After stretch-induced injury treatment, the apoptosis of CHIP-OE cells and the CHIP-knockdown (shRNA1 and shRNA4) cells were detected using FACS analysis (**Figure 2B**). The results showed that CHIP-OE slightly attenuated cell apoptosis of bEnd.3 cells after stretch-induced injury treatment; the apoptosis rates of normal control (NC)-OE cells and CHIP-OE were 1.991 and 0.072%, respectively ($p < 0.01$), whereas the cell apoptosis of injured bEnd.3 cells was induced after CHIP interference (shRNA1 and shRNA4 groups) (**Figures 2B–D**). Compared with the apoptosis rate

(0.498%) of NC-shRNA cells, the apoptosis rates of shRNA1 and shRNA4 cells were significantly increased, which were 86.915 and 79.148%, respectively ($p < 0.01$). This result was well coordinated with the bright field image in **Figure 1A**. Above all, CHIP-OE promoted cell proliferation and attenuated cell apoptosis after stretch-induced injury treatment.

## C Terminus of Hsc70-Interacting Protein Overexpression Enhanced Cell Migration and Cell Invasion After *in vitro* Simulated Traumatic Brain Injury

Transwell assay was used to detect bEnd.3 cell invasion after stretch-induced injury treatment *in vitro*; the results showed that CHIP-OE enhanced cell invasion, whereas CHIP interference weakened the cell invasion of injured bEnd.3 cells (**Figures 3A,B**). Wound healing test was adopted to detect bEnd.3 cell migration after stretch-induced injury treatment *in vitro*; the results showed that CHIP-OE enhanced cell migration, whereas CHIP interference weakened the cell migration of injured bEnd.3 cells (**Figures 3C,D**). Above all, brain injury results in permanent damage and scar formation; the fact that CHIP-OE promoted cell migration and cell invasion after stretch-induced injury implies that CHIP may be a crucial molecule to augment recovery of brain injury after TBI.

**FIGURE 2 |** C terminus of Hsc70-interacting protein (CHIP) overexpression promoted bEnd.3 cell growth after stretch-induced injury treatment. **(A)** CCK-8 assay was used to determine bEnd.3 cell viability. Cells were seeded in Bioflex 6-well plates for 12 h, followed by *in vitro* stretch-induced injury treatment. After 6, 24, 48, and 72 h, optical density (OD) value was measured at 450 nm. Experiment was performed in triplicate at different times. \*\**p* < 0.01 vs. the NC-OE, ##*p* < 0.01 vs. the NC-shRNA. **(B)** Cells were seeded in Bioflex 6-well plates for 24 h, followed by *in vitro* stretch-induced injury treatment. $5 \times 10^5$/ml treated cells were treated and analyzed by fluorescence-activated cell sorting cytometry. For each sample, at least 10,000 cells were analyzed. **(C,D)** Quantitative statistics of apoptosis rate. \*\*\**p* < 0.001 vs. the NC-OE, ###*p* < 0.001 vs. the NC-shRNA.

## C Terminus of Hsc70-Interacting Protein Overexpression Downregulated Apoptosis and Procoagulant Molecules After *in vitro* Simulated Traumatic Brain Injury

The immunoblotting results showed that CHIP-OE downregulated PTEN protein level, inducing activation of AKT, and CHIP interference upregulated PTEN protein level, preventing activation of AKT in bEnd.3 cells after stretch injury (**Figures 4A,B**). **Figure 4** also showed that CHIP-OE downregulated downstream apoptosis molecules like cleaved caspase3, cleaved caspase8, Fas, and apoptosis-inducing factor, which was consistent with the previous result that CHIP-OE attenuated cell apoptosis after stretch-induced injury treatment. As for downstream procoagulant molecules such as TF, vWF, PECAM-1, and PAI-1, they were downregulated by the CHIP-OE (**Figures 4C,D**), which gave us a hint that CHIP-OE might suppress coagulation after stretch injury through inhibiting

activation of those procoagulant molecules. The ubiquitination assay results showed that CHIP-OE significantly improved PTEN ubiquitination (**Figure 4G**). Combined with the discussed results, CHIP-OE downregulated apoptosis and procoagulant molecules to suppress cell apoptosis and coagulation after stretch-induced injury treatment, which seems to be mediated through PTEN ubiquitination and AKT activation.

## C Terminus of Hsc70-Interacting Protein Overexpression Downregulated Apoptosis and Procoagulant Molecules After *in vivo* Traumatic Brain Injury

According to the interfere effect of shRNA targeting CHIP, lentiviral particles of shRNA4 were used in animal study. CCI injury was adopted as *in vivo* TBI treatment. CHIP-OE and interference lentiviruses were injected through lateral cerebral ventricle injection. Immunoblotting results showed that CHIP-OE induced AKT activation, whereas CHIP interference

**FIGURE 3 |** C terminus of Hsc70-interacting protein (CHIP) overexpression enhanced cell migration and cell invasion after *in vitro* simulated traumatic brain injury. **(A)** Invasion capacity of the cells was evaluated by the transwell assay. Cells were stained with crystal violet and counted in five randomly selected microscopic fields. **(B)** Quantitative statistics of invasion capacity. **$p < 0.01$ vs. the NC-OE, #$p < 0.05$ vs. the NC-shRNA. **(C)** Migration capacity of the cells was evaluated by the wound healing test. $3 \times 10^5$ cells were seeded in the Bioflex 6-well plates for 12 h, followed by *in vitro* stretch-induced injury treatment. Wound healing was observed after 0, 24, and 48 h within the scrape line, and representative scrape lines were imaged. **(D)** Quantitative statistics of migration capacity. *$p < 0.05$ vs. the NC-OE, #$p < 0.05$ vs. the NC-shRNA. Scale bars: 50 μm.

upregulated PTEN protein level and suppressed AKT activation in the pericontusional cortex of mice subjected to CCI (**Figure 5A**). CHIP-OE also downregulated apoptosis and procoagulant molecules in the pericontusional areas after *in vivo* TBI (**Figure 5B**), which was consistent with the result *in vitro*. Thus, the regulation of CHIP may suppress TBI-induced apoptosis and procoagulant activity through PTEN/AKT signaling pathway.

## C Terminus of Hsc70-Interacting Protein Overexpression Promoted Microvascular and Blood–Brain Barrier Repair After *in vivo* Traumatic Brain Injury

Immunofluorescence results demonstrated that CHIP-OE significantly increased CD31 expression levels during the early phase of TBI, but there appeared a significant decrease trend in the CHIP interference group (**Figure 6**), which implied that CHIP upregulation may strengthen the formation of cerebral microvessels after TBI. The hematoxylin and eosin staining results showed rupture of cerebral microvessels and scattered hemorrhage in the pericontusional cortex after TBI, and the hemorrhagic injuries in the pericontusional regions reduced continuously in the CHIP-OE group during the acute phase of

TBI (**Figures 7A–C**). Moreover, a significant time-dependent decrease of TBI-induced IgG leakage was also found in the CHIP-OE group, which indicated that the upregulation of CHIP may be conducive to decreasing BBB permeability and maintaining BBB integrity after TBI (**Figures 7D–F**). All the discussed results indicated that CHIP-OE may contribute to microvascular and BBB repair after TBI.

## DISCUSSION

Clinical risk factors or predictors studies showed that TIC closely related with PHI and PTCI (Tian et al., 2010; Yuan et al., 2012; Chen et al., 2013; Maegele, 2013; Yang et al., 2014; de Oliveira Manoel et al., 2015; Liu and Tian, 2016), which implied that TBI can break the dynamic balance between procoagulant and fibrinolytic systems to promote coagulation disorder, and it might be the important contributor to the initiation of pathological cascade secondary injury processes, including progressive hemorrhagic and ischemic brain injuries. The mechanism of TIC in TBI has not been fully elucidated, and PTEN is speculated to play a crucial role in the development of coagulation disorder after TBI. In this study, we first used lentivirus-mediated gene transfection technique to regulate CHIP
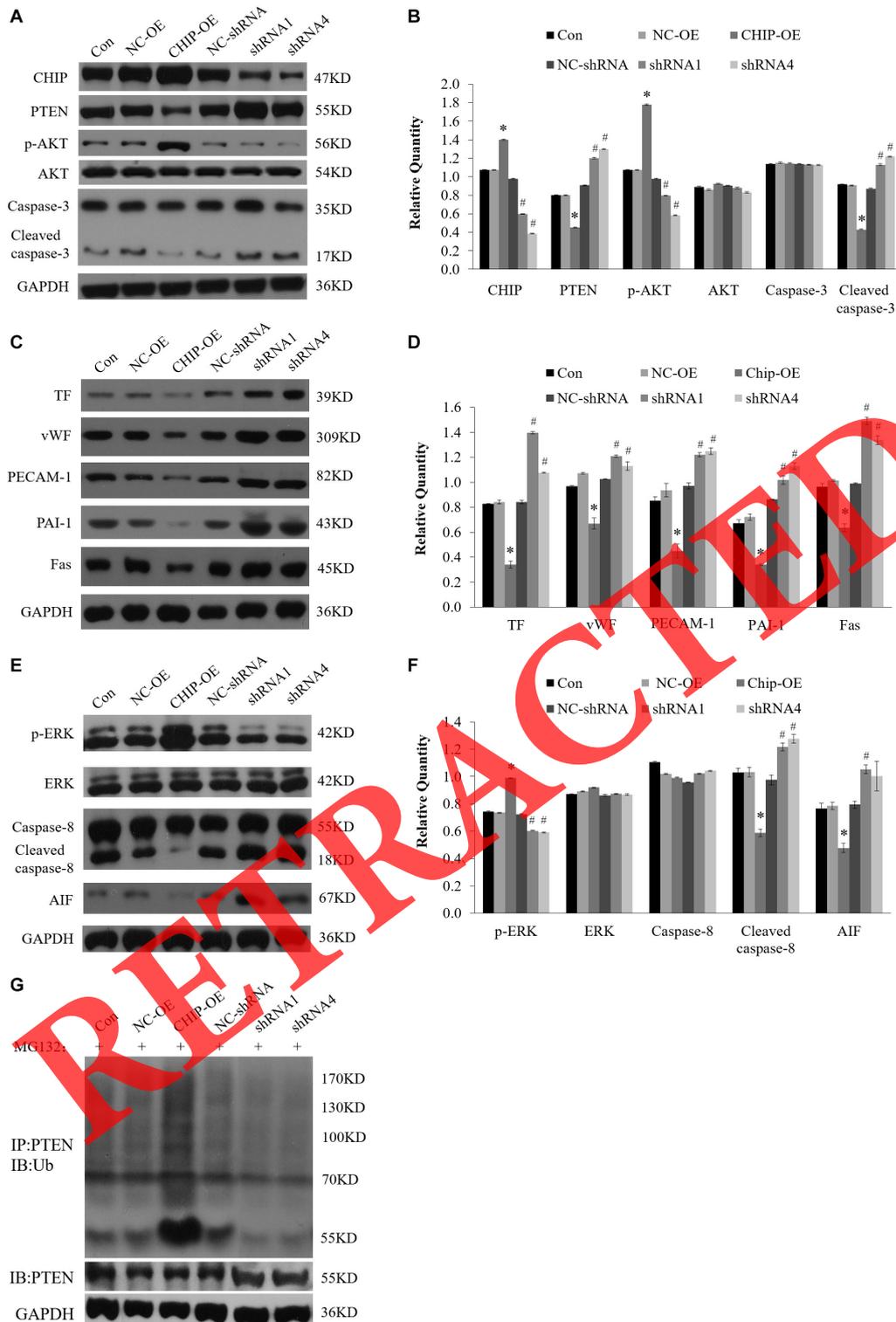
**FIGURE 4 |** C terminus of Hsc70-interacting protein (CHIP) overexpression attenuated procoagulant and apoptosis molecule expressions after *in vitro* simulated traumatic brain injury. **(A,C,E)** Changes of CHIP, PTEN, procoagulant molecules, and apoptosis molecules after *in vitro* stretch-induced injury treatment. ERK contains ERK1 and ERK2 with the molecular mass of 38–44 kDa; here, the bands of ERK1 and ERK2 were scanned and quantified together as p-ERK/ERK. **(B,D,F)** Relevant grayscale scanning analysis results of CHIP, PTEN, procoagulant molecules, and apoptosis molecules after *in vitro* stretch-induced injury treatment. **(G)** After treatment of MG132 for 12 h, PTEN immunoprecipitation products were tested with immunoblotting. Quantification of proteins was normalized to glyceraldehyde-3-phosphate dehydrogenase. *$p < 0.05$ vs. the NC-OE, #$p < 0.05$ vs. the NC-shRNA.
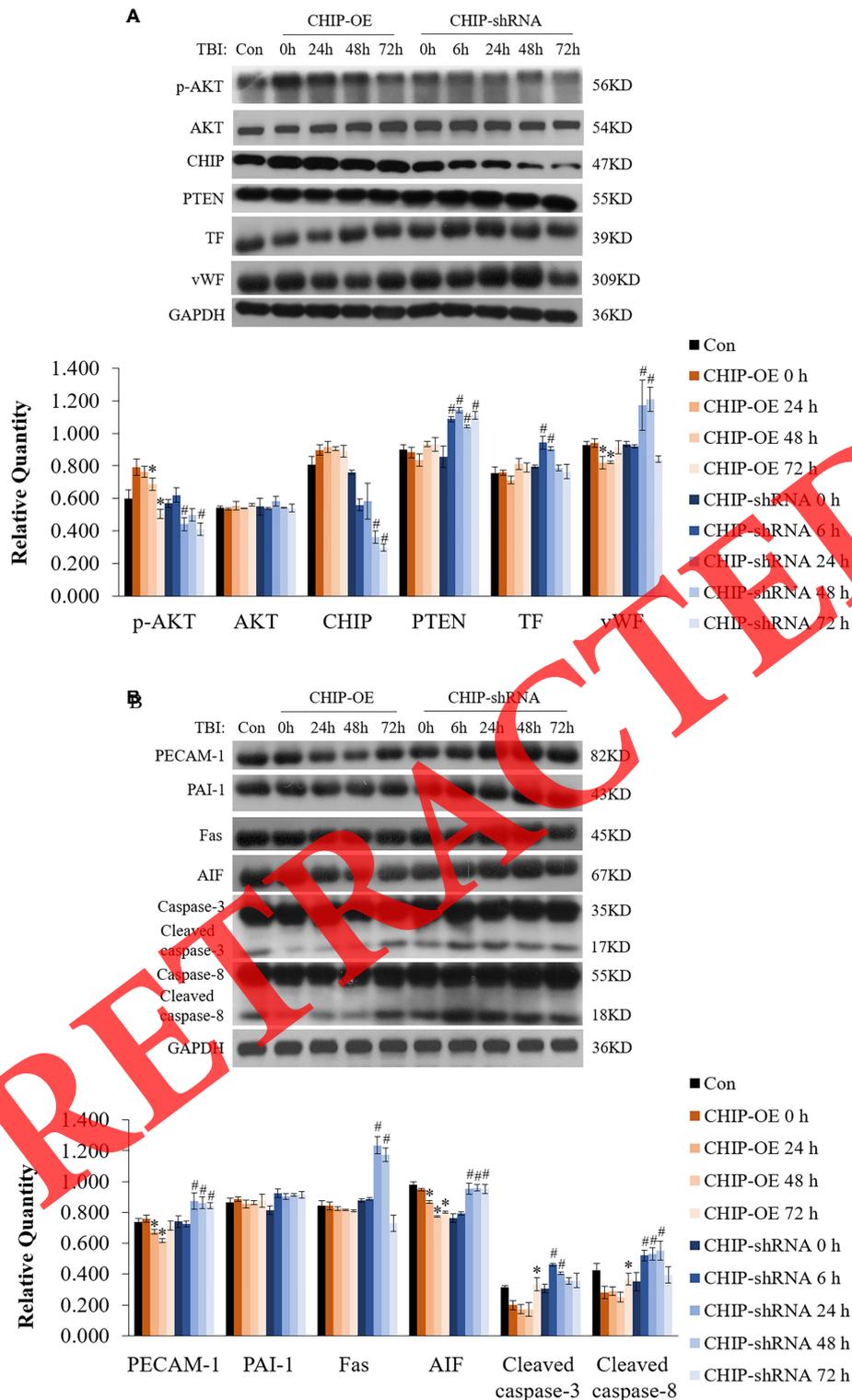
**FIGURE 5 |** C terminus of Hsc70-interacting protein (CHIP) overexpression suppressed procoagulant and apoptosis molecule expressions in pericontusional areas after *in vivo* traumatic brain injury (TBI). All groups were experienced with *in vivo* TBI treatment. CHIP-OE group of mice were killed after 0, 24, 48, and 72 h of CCI, and CHIP-shRNA group of mice were killed after 0, 6, 24, 48, and 72 h of CCI. Three-millimeter coronal tissue section from the ipsilateral cortex centering on the impact site was obtained immediately after killing. **(A)** Changes of CHIP, PTEN, and p-AKT levels in each group after *in vivo* TBI. **(B)** Changes of procoagulant molecules and apoptosis molecules in each group after *in vivo* TBI. Quantification of proteins was normalized to glyceraldehyde-3-phosphate dehydrogenase. *$p < 0.05$ vs. the CHIP-OE-0h, #$p < 0.05$ vs. the CHIP-shRNA-0 h.
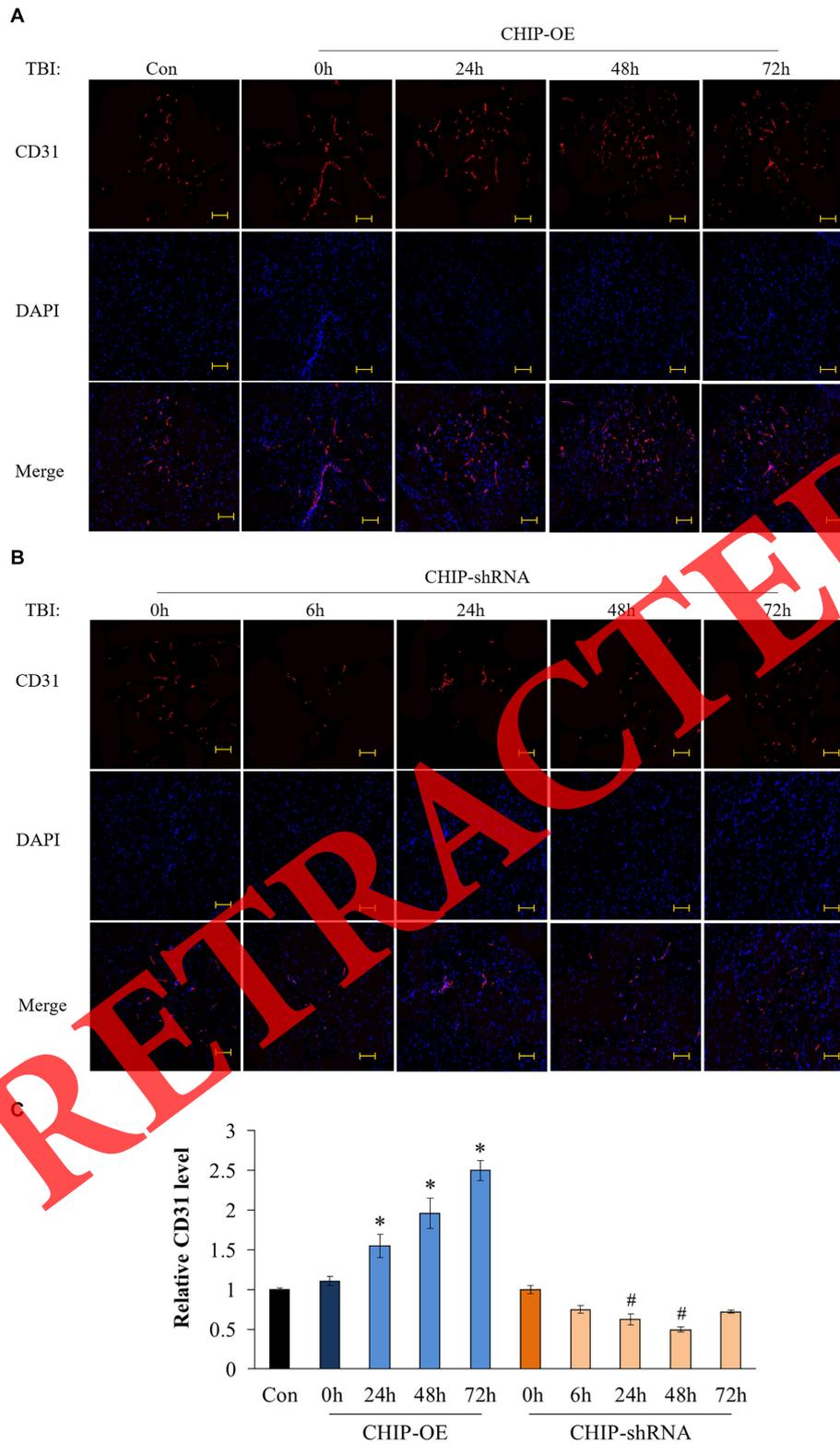
**FIGURE 6 |** C terminus of Hsc70-interacting protein (CHIP) overexpression increased micrangium density in pericontusional areas after *in vivo* traumatic brain injury. **(A)** Immunofluorescence results of CD31 in pericontusional cortex after 0, 24, 48, and 72 h of CCI in CHIP-OE group. **(B)** Immunofluorescence results of CD31 in pericontusional cortex after 0, 6, 24, 48, and 72 h of CCI in CHIP-shRNA group. **(C)** Relative expression levels of CD31. CHIP-OE 24, 48, and 72 h vs. CHIP-OE-0h, *$p < 0.05$; CHIP-shRNA 6, 24, 48, and 72 h vs. CHIP-shRNA-0h, #$p < 0.05$. Scale bars: 50 μm.

**FIGURE 7 |** Hematoxylin and eosin (HE) staining and blood–brain barrier permeability evaluation after *in vivo* traumatic brain injury. **(A)** HE staining (40×) in pericontusional cortex at 0, 24, 48, and 72 h after CCI in CHIP-OE group. **(B)** HE staining (40×) in pericontusional cortex at 0, 6, 24, 48, and 72 h after CCI in CHIP-shRNA group. **(C)** Semi-quantified analysis of hemorrhagic injury (red stained areas) using mean OD. CHIP-OE 24, 48, and 72 h vs. CHIP-OE-0h, ***$p < 0.001$; CHIP-shRNA 6, 24, 48, and 72 h vs. CHIP-shRNA-0 h, ##$p < 0.01$, ###$p < 0.001$. **(D)** Immunohistochemical staining (200×) of IgG leakage in pericontusional regions at 0, 24, 48, and 72 h after CCI in CHIP-OE group. **(E)** Immunohistochemical staining (200×) of IgG leakage in pericontusional regions at 0, 6, 24, 48, and 72 h after CCI in CHIP-shRNA group. **(F)** Semi-quantitative analysis of leaked IgG protein using mean OD. CHIP-OE 24, 48, and 72 h vs. CHIP-OE-0h, ***$p < 0.001$; CHIP-shRNA 6, 24, 48, and 72 h vs. CHIP-shRNA-0 h, ###$p < 0.001$. Scale bars in **(A,B)** were 200 μm and, in **(D,E)**, were 50 μm.

expression, which is considered to regulate the ubiquitination level and proteasomal turnover of PTEN. Meanwhile, *in vitro* simulated TBI model and *in vivo* TBI model were established using stretch-induced injury on cells and CCI injury on mice, as we reported previously (Xu Z. M. et al., 2017; Liu et al., 2018; Yang et al., 2019). Our study demonstrated that upregulation of CHIP expression facilitated BMVEC proliferation, migration, and invasion but attenuated cell apoptosis and downregulated the expressions of procoagulant molecules after stretch-induced injury treatment. Further *in vivo* experiments also indicated that CHIP-OE suppressed post-TBI apoptosis, procoagulant activity, increased microvessel density, and reduced hemorrhagic injury and BBB permeability in the pericontusion areas. Notably, all findings suggested that CHIP-induced apoptosis and procoagulation resistance, as well as brain injury repair may be closely associated with PTEN/AKT signaling pathway in TBI.

As a major negative regulator, PTEN has been confirmed to be involved in the activation of AKT signaling after cerebral ischemia and TBI (Liu et al., 2010; Ding et al., 2013; Guo et al., 2013; Kitagishi and Matsuda, 2013; Wang et al., 2013; Kilic et al., 2017; Xue et al., 2018), and PTEN phosphorylation could reduce the apoptosis of neurons and the permeability of BBB and may contribute to neuroprotection after TBI (Hasegawa et al., 2012; Ding et al., 2013; Kitagishi and Matsuda, 2013; Wang et al., 2013). However, the impact of other post-translational

modification of PTEN on TBI has not been elucidated. In this study, we found that CHIP-OE induced PTEN ubiquitination and maintained PTEN turnover, in accordance with a previous report (Ahmed et al., 2012). We found an enhancement of PTEN ubiquitination and substantial decrease of PTEN protein level, as well as AKT activation after CHIP-OE. AKT signal is known to regulate multiple biological processes including cell survival, proliferation, growth, and glycogen metabolism. It has been reported that CHIP-induced apoptosis resistance is closely associated with the AKT signaling pathway in breast cancer cells and tissues (Lv et al., 2013). This finding is supported by our study that showed a same antiapoptosis effects of CHIP-OE in bEnd.3 cells against TBI. Furthermore, bEnd.3 cell proliferation, migration, and invasion were also promoted by CHIP-OE, which are helpful in improving BBB repair after TBI. Generally, BBB is formed primarily by BMVECs, so the recovery of BMVECs function is the key to BBB repair after TBI. The significance of this finding is substantiated by the *in vivo* evidence that BBB permeability was decreased significantly after CHIP-OE. Therefore, CHIP upregulation might be considered as a potential protective strategy in microvascular endothelial injury and preservation of the BBB function after TBI.

Hypercoagulation is a common complication after severe TBI, which frequently leads to major secondary injuries like deep venous thrombosis, PTCI, and even acute pulmonary

embolism (Chen et al., 2013; Maegele, 2013). However, it remains to be controversial whether anticoagulation treatment should be started during the early phase of TBI due to the increasing potential risk for progressive hemorrhagic injures. Although the evidence to determine when to anticoagulate is still limited, initiating preventive measures should be necessary to reduce occurrences of thrombotic events. After TBI, increasing procoagulant activity can shift the balance of procoagulant and anticoagulant reactions on the vascular endothelium, which is ultimately a hypercoagulable state. Our study demonstrated that CHIP-OE may suppress coagulation cascade through inhibiting expression of procoagulant molecules involved in the early phase of TBI (TF, vWF, PECAM-1, and PAI-1), which is possibly associated with the activation of the PTEN/AKT signaling. Furthermore, we also found that the density of capillaries was increased significantly in the brain tissue surrounding the contusion area after CHIP-OE, whereas hemorrhagic tendency was decreased more obviously, which suggested that CHIP-induced PTEN inhibition may attenuate progression of the secondary hemorrhagic injuries and stimulate microvascular regeneration. Interestingly, our recent research proposed that PTEN inhibition promoted post-ischemic angiogenesis *in vitro*, and this enhancing effect might also be achieved through activation of the AKT signal cascade (Xue et al., 2018), which is consistent with a recent report. An ovarian cancer study by He et al. (2019) showed that miR-205 could induce angiogenesis by silencing PTEN and subsequently activates AKT pathway, whereas restoring of PTEN expression can rescue the suppression of angiogenesis induced by the miR-205 inhibitor. Thus, the PTEN/AKT pathway may play a crucial role in the vascular repair and remodeling after TBI and cerebral ischemia.

In general, CHIP is a ubiquitously expressed cochaperone and has a Ubox-dependent E3 ligase activity; PTEN is its downstream target, which could be ubiquitinated by CHIP. Our study demonstrated that CHIP-OE or silencing regulates procoagulation activity and microvascular and BBB repair after TBI, and this may be achieved through PTEN/AKT pathway. Nevertheless, it is premature to conclude that CHIP upregulation attenuates TBI-induced coagulopathy because the effects of CHIP on blood coagulation in mice were not investigated in this study. Notably, the existence of a real feedback loop between PTEN and the AKT signaling pathway remains undetermined and thus needs to be clarified in the future studies. Additionally, whether other cascades downstream to PTEN contributes to attenuating coagulation disorder and neuroprotective effect against TBI needs further investigated. Finally, other potential targets of CHIP-mediated ubiquitination may also be involved in the

apoptosis, procoagulation, and microvascular and BBB repair, which also need further research.

## CONCLUSION

In this study, CHIP is shown to attenuate apoptosis and procoagulant activity and facilitate microvascular and BBB repair during the early phase of TBI. The upregulation of CHIP may improve the recovery of BMVEC function and promote brain repair after TBI, which provides a novel treatment strategy for TBI.

## DATA AVAILABILITY STATEMENT

The datasets generated for this study are available on request to the corresponding author.

## ETHICS STATEMENT

The animal study was reviewed and approved by the Shanghai Jiao Tong University Affiliated Sixth People's Hospital.

## AUTHOR CONTRIBUTIONS

HC and LX designed the study. HC, YJ, and ZX performed the experiments. HC, YJ, and DY collected and analyzed the data. SJ and YG searched and reviewed the literatures. HC drafted the article. HT and LX critically revised the article. LX approved the final version of the manuscript on behalf of all authors. All authors contributed to the article and approved the submitted version.

## REFERENCES

Ahmed, S. F., Deb, S., Paul, I., Chatterjee, A., Mandal, T., Chatterjee, U., et al. (2012). The chaperone-assisted E3 ligase C terminus of Hsc70-interacting protein (CHIP) targets PTEN for proteasomal degradation. *J. Biol. Chem.* 287, 15996–16006. doi: 10.1074/jbc.M111.321083

Barklin, A., Tonnesen, E., Ingerslev, J., Sorensen, B., and Fenger-Eriksen, C. (2009). Coagulopathy during induced severe intracranial hypertension in

a porcine donor model. *Anesthesiology* 110, 1287–1292. doi: 10.1097/ALN. 0b013e3181a10352

Carlos, T. M., Clark, R. S., Franicola-Higgins, D., Schiding, J. K., and Kochanek, P. M. (1997). Expression of endothelial adhesion molecules and recruitment of neutrophils after traumatic brain injury in rats. *J. Leukoc. Biol.* 61, 279–285. doi: 10.1002/jlb.61.3.279

Carrick, M. M., Tyroch, A. H., Youens, C. A., and Handley, T. (2005). Subsequent development of thrombocytopenia and coagulopathy in moderate and severe

head injury: support for serial laboratory examination. *J. Trauma* 58, 725–730. doi: 10.1097/01.ta.0000159249.68363.78

Chen, H., Xue, L. X., Guo, Y., Chen, S. W., Wang, G., Cao, H. L., et al. (2013). The influence of hemocoagulation disorders on the development of posttraumatic cerebral infarction and outcome in patients with moderate or severe head trauma. *Biomed Res. Int.* 2013:685174. doi: 10.1155/2013/685174

Condron, M., Rowell, S., Dewey, E., Anderson, T., Lealiiee, L., Farrell, D., et al. (2018). The procoagulant molecule plasminogen activator inhibitor-1 is associated with injury severity and shock in patients with and without traumatic brain injury. *J. Trauma Acute Care Surg.* 85, 888–893. doi: 10.1097/TA.0000000000002040

De Luca, C., Virtuoso, A., Maggio, N., and Papa, M. (2017). Neuro-coagulopathy: blood coagulation factors in central nervous system diseases. *Int. J. Mol. Sci.* 18:2128. doi: 10.3390/ijms18102128

De Oliveira, C. O., Reimer, A. G., Da Rocha, A. B., Grivicich, I., Schneider, R. F., Roisenberg, I., et al. (2007). Plasma von Willebrand factor levels correlate with clinical outcome of severe traumatic brain injury. *J. Neurotrauma* 24, 1331–1338. doi: 10.1089/neu.2006.0159

de Oliveira Manoel, A. L., Neto, A. C., Veigas, P. V., and Rizoli, S. (2015). Traumatic brain injury associated coagulopathy. *Neurocrit. Care* 22, 34–44. doi: 10.1007/s12028-014-0026-4

Ding, J., Guo, J., Yuan, Q., Yuan, F., Chen, H., and Tian, H. (2013). Inhibition of phosphatase and tensin homolog deleted on chromosome 10 decreases rat cortical neuron injury and blood-brain barrier permeability, and improves neurological functional recovery in traumatic brain injury model. *PLoS One* 8:e80429. doi: 10.1371/journal.pone.0080429

Ellis, E. F., McKinney, J. S., Willoughby, K. A., Liang, S., and Povlishock, J. T. (1995). A new model for rapid stretch-induced injury of cells in culture: characterization of the model using astrocytes. *J. Neurotrauma* 12, 325–339. doi: 10.1089/neu.1995.12.325

Ge, X. T., Lei, P., Wang, H. C., Zhang, A. L., Han, Z. L., Chen, X., et al. (2014). miR-21 improves the neurological outcome after traumatic brain injury in rats. *Sci. Rep.* 4:6718. doi: 10.1038/srep06718

Guo, J. Y., Ding, J., Yuan, F., Chen, H., Chen, S. W., and Tian, H. L. (2013). Dose-dependent protective effect of bisperoxovanadium against acute cerebral ischemia in a rat model of ischemia/reperfusion injury. *Int. J. Mol. Sci.* 14, 12013–12022. doi: 10.3390/ijms140612013

Han, Z., Chen, F., Ge, X., Tan, J., Lei, P., and Zhang, J. (2014). miR-21 alleviated apoptosis of cortical neurons through promoting PTEN-Akt signaling pathway in vitro after experimental traumatic brain injury. *Brain Res.* 1582, 12–20. doi: 10.1016/j.brainres.2014.07.045

Hasegawa, Y., Suzuki, H., Altay, O., Chen, H., and Zhang, J. H. (2012). Treatment with sodium orthovanadate reduces blood-brain barrier disruption via phosphatase and tensin homolog deleted on chromosome 10 (PTEN) phosphorylation in experimental subarachnoid hemorrhage. *J. Neurosci. Res.* 90, 691–697. doi: 10.1002/jnr.22801

He, L., Zhu, W., Chen, Q., Yuan, Y., Wang, Y., Wang, J., et al. (2019). Ovarian cancer cell-secreted exosomal miR-205 promotes metastasis by inducing angiogenesis. *Theranostics* 9, 8206–8220. doi: 10.7150/thno.37455

Hori, Y., Nakatani, K., Morioka, K., Katsuki, A., Gabazza, E. C., Yano, Y., et al. (2005). Insulin enhanced thrombin-activable fibrinolysis inhibitor expression through PI3 kinase/Akt pathway. *Int. J. Mol. Med.* 15, 265–268.

Kao, S. H., Wu, H. T., and Wu, K. J. (2018). Ubiquitination by HUWE1 in tumorigenesis and beyond. *J. Biomed. Sci.* 25:67. doi: 10.1186/s12929-018-0470-0

Kilic, U., Caglayan, A. B., Beker, M. C., Gunal, M. Y., Caglayan, B., Yalcin, E., et al. (2017). Particular phosphorylation of PI3K/Akt on Thr308 via PDK-1 and PTEN mediates melatonin's neuroprotective activity after focal cerebral ischemia in mice. *Redox Bio.* 12, 657–665. doi: 10.1016/j.redox.2017.04.006

Kitagishi, Y., and Matsuda, S. (2013). Diets involved in PPAR and PI3K/AKT/PTEN pathway may contribute to neuroprotection in a traumatic brain injury. *Alzheimers Res. Ther.* 5:42. doi: 10.1186/alzrt208

Liu, C., Wu, J., Xu, K., Cai, F., Gu, J., Ma, L., et al. (2010). Neuroprotection by baicalein in ischemic brain injury involves PTEN/AKT pathway. *J. Neurochem.* 112, 1500–1512. doi: 10.1111/j.1471-4159.2009.06561.x

Liu, J., and Tian, H. L. (2016). Relationship between trauma-induced coagulopathy and progressive hemorrhagic injury in patients with traumatic brain injury. *Chin. J. Traumatol.* 19, 172–175. doi: 10.1016/j.cjtee.2016.01.011

Liu, S., Wan, X., Wang, S., Huang, L., Zhu, M., Zhang, S., et al. (2015). Posttraumatic cerebral infarction in severe traumatic brain injury: characteristics, risk factors and potential mechanisms. *Acta Neurochir.* 157, 1697–1704. doi: 10.1007/s00701-015-2559-5

Liu, Y. L., Yuan, F., Yang, D. X., Xu, Z. M., Jing, Y., Yang, G. Y., et al. (2018). Adjudin attenuates cerebral edema and improves neurological function in mice with experimental traumatic brain injury. *J. Neurotrauma* 35, 2850–2860. doi: 10.1089/neu.2017.5397

Lv, Y., Song, S., Zhang, K., Gao, H., and Ma, R. (2013). CHIP regulates AKT/FoxO/Bim signaling in MCF7 and MCF10A cells. *PLoS One* 8:e83312. doi: 10.1371/journal.pone.0083312

Maegele, M. (2013). Coagulopathy after traumatic brain injury: incidence, pathogenesis, and treatment options. *Transfusion* 53, 28S–37S. doi: 10.1111/trf.12033

Marino, R., Gasparotti, R., Pinelli, L., Manzoni, D., Gritti, P., Mardighian, D., et al. (2006). Posttraumatic cerebral infarction in patients with moderate or severe head trauma. *Neurology* 67, 1165–1171. doi: 10.1212/01.wnl.0000238081.35281.b5

McKinney, J. S., Willoughby, K. A., Liang, S., and Ellis, E. F. (1996). Stretch-induced injury of cultured neuronal, glial, and endothelial cells. Effect of polyethylene glycol-conjugated superoxide dismutase. *Stroke* 27, 934–940. doi: 10.1161/01.str.27.5.934

Morel, N., Morel, O., Petit, L., Hugel, B., Cochard, J. F., Freyssinet, J. M., et al. (2008). Generation of procoagulant microparticles in cerebrospinal fluid and peripheral blood after traumatic brain injury. *J. Trauma* 64, 698–704. doi: 10.1097/TA.0b013e31816493ad

Schabbauer, G., Tencati, M., Pedersen, B., Pawlinski, R., and Mackman, N. (2004). PI3K-Akt pathway suppresses coagulation and inflammation in endotoxemic mice. *Arterioscler. Thromb. Vasc. Biol.* 24, 1963–1969. doi: 10.1161/01.ATV.0000143096.15099.ce

Schwarzmaier, S. M., Kim, S. W., Trabold, R., and Plesnila, N. (2010). Temporal profile of thrombogenesis in the cerebral microcirculation after traumatic brain injury in mice. *J. Neurotrauma* 27, 121–130. doi: 10.1089/neu.2009.1114

Server, A., Dullerud, R., Haakonsen, M., Nakstad, P. H., Johnsen, U. L., and Magnaes, B. (2001). Post-traumatic cerebral infarction. Neuroimaging findings, etiology and outcome. *Acta Radiol.* 42, 254–260. doi: 10.1034/j.1600-0455.2001.042003254.x

Shao, G., Li, Z., Ahmad, N., and Liu, X. (2017). Regulation of PTEN degradation and NEDD4-1 E3 ligase activity by Numb. *Cell Cycle* 16, 957–967. doi: 10.1080/15384101.2017.1310351

Song, M. S., Salmena, L., and Pandolfi, P. P. (2012). The functions and regulation of the PTEN tumour suppressor. *Nat. Rev. Mol. Cell Biol.* 13, 283–296. doi: 10.1038/nrm3330

Stein, S. C., Graham, D. I., Chen, X. H., and Smith, D. H. (2004). Association between intravascular microthrombosis and cerebral ischemia in traumatic brain injury. *Neurosurgery* 54, 687–691. doi: 10.1227/01.neu.0000108641.98845.88

Stein, S. C., Spettell, C., Young, G., and Ross, S. E. (1993). Delayed and progressive brain injury in closed-head trauma: radiological demonstration. *Neurosurgery* 32, 30–21. doi: 10.1227/00006123-199301000-00004

Stein, S. C., Young, G. S., Talucci, R. C., Greenbaum, B. H., and Ross, S. E. (1992). Delayed brain injury after head trauma: significance of coagulopathy. *Neurosurgery* 30, 160–165. doi: 10.1227/00006123-199202000-00002

Tawil, I., Stein, D. M., Mirvis, S. E., and Scalea, T. M. (2008). Posttraumatic cerebral infarction: incidence, outcome, and risk factors. *J. Trauma* 64, 849–853. doi: 10.1097/TA.0b013e318160c08a

Tian, H. L., Chen, H., Wu, B. S., Cao, H. L., Xu, T., Hu, J., et al. (2010). D-dimer as a predictor of progressive hemorrhagic injury in patients with traumatic brain injury: analysis of 194 cases. *Neurosurg. Rev.* 33, 359–365. doi: 10.1007/s10143-010-0251-z

Tian, H. L., Geng, Z., Cui, Y. H., Hu, J., Xu, T., Cao, H. L., et al. (2008). Risk factors for posttraumatic cerebral infarction in patients with moderate or severe head trauma. *Neurosurg. Rev.* 31, 431–437. doi: 10.1007/s10143-008-0153-5

Voutsadakis, I. A. (2012). The ubiquitin-proteasome system and signal transduction pathways regulating Epithelial Mesenchymal transition of cancer. *J. Biomed. Sci.* 19:67. doi: 10.1186/1423-0127-19-67

Wang, G., Jiang, X., Pu, H., Zhang, W., An, C., Hu, X., et al. (2013). Scriptaid, a novel histone deacetylase inhibitor, protects against traumatic brain injury

via modulation of PTEN and AKT pathway : scriptaid protects against TBI via AKT. *Neurotherapeutics* 10, 124–142. doi: 10.1007/s13311-012-0157-2

Xu, T., Wang, H., Jiang, M., Yan, Y., Li, W., Xu, H., et al. (2017). The E3 ubiquitin ligase CHIP/miR-92b/PTEN regulatory network contributes to tumorigenesis of glioblastoma. *Am. J. Cancer Res.* 7, 289–300.

Xu, Z. M., Yuan, F., Liu, Y. L., Ding, J., and Tian, H. L. (2017). Glibenclamide Attenuates Blood-Brain Barrier Disruption in Adult Mice after Traumatic Brain Injury. *J. Neurotrauma* 34, 925–933. doi: 10.1089/neu.2016. 4491

Xue, L., Huang, J., Zhang, T., Wang, X., Fu, J., Geng, Z., et al. (2018). PTEN inhibition enhances angiogenesis in an in vitro model of ischemic injury by promoting Akt phosphorylation and subsequent hypoxia inducible factor-1alpha upregulation. *Metab. Brain Dis.* 33, 1679–1688. doi: 10.1007/s11011-018-0276-5

Yang, D. B., Yu, W. H., Dong, X. Q., Du, Q., Shen, Y. F., Zhang, Z. Y., et al. (2014). Plasma copeptin level predicts acute traumatic coagulopathy and progressive hemorrhagic injury after traumatic brain injury. *Peptides* 58, 26–29. doi: 10. 1016/j.peptides.2014.05.015

Yang, D. X., Jing, Y., Liu, Y. L., Xu, Z. M., Yuan, F., Wang, M. L., et al. (2019). Inhibition of transient receptor potential vanilloid 1 attenuates blood-brain barrier disruption after traumatic brain injury in mice. *J. Neurotrauma* 36, 1279–1290. doi: 10.1089/neu.2018.5942

Yuan, F., Ding, J., Chen, H., Guo, Y., Wang, G., Gao, W. W., et al. (2012). Predicting progressive hemorrhagic injury after traumatic brain injury: derivation and validation of a risk score based on admission characteristics. *J. Neurotrauma* 29, 2137–2142. doi: 10.1089/neu.2011.2233

Yuan, F., Xu, Z. M., Lu, L. Y., Nie, H., Ding, J., Ying, W. H., et al. (2016). SIRT2 inhibition exacerbates neuroinflammation and blood-brain barrier disruption in experimental traumatic brain injury by enhancing NF-kappaB p65 acetylation and activation. *J. Neurochem.* 136, 581–593. doi: 10.1111/jnc.13423

Zhang, J., Jiang, R., Liu, L., Watkins, T., Zhang, F., and Dong, J. F. (2012). Traumatic brain injury-associated coagulopathy. *J. Neurotrauma* 29, 2597–2605. doi: 10.1089/neu.2012.2348